ADVANCED FUNCTIONAL MATERIALS
www.afm-journal.de

Thermoresponsive Shape-Memory Hydrogel Actuators Made by Phototriggered Click Chemistry

*Binoy Maiti, Alex Abramov, Lourdes Franco, Jordi Puiggalí, Hamidreza Enshaei, Carlos Alemán, and David Díaz Díaz**

Dedicated to the memory of Professor Catalina Ruiz-Pérez

This article describes the design and synthesis of a new series of hydrogel membranes composed of trialkyne derivatives of glycerol ethoxylate and bisphenol A diazide (BA-diazide) or diazide-terminated PEG600 monomer via a Cu(I)-catalyzed photoclick reaction. The water-swollen hydrogel membranes display thermoresponsive actuation and their lower critical solution temperature (LCST) values are determined by differential scanning calorimetry. Glycerol ethoxylate moiety serves as the thermoresponsive component and hydrophilic part, while the azide-based component acts as the hydrophobic comonomer and most likely provides a critical hydrophobic/hydrophilic balance contributing also to the significant mechanical strength of the membranes. These hydrogels exhibit a reversible shape-memory effect in response to temperature through a defined phase transition. The swelling and deswelling behavior of the membranes are systematically examined. Due to the click nature of the reaction, easy availability of azide and alkyne functional-monomers, and the polymer architecture, the glass transition temperature (T_g) is easily controlled through monomer design and crosslink density by varying the feed ratio of different monomers. The mechanical properties of the membranes are studied by universal tensile testing measurements. Moreover, the hydrogels show the ability to absorb a dye and release it in a controlled manner by applying heat below and above the LCST.

1. Introduction

Stimuli-responsive polymers have received much attention over the years due to their biomimetic behavior and diverse range of potential applications in different fields, such as drug delivery[1,2,3] tissue engineering,[4] biosensing,[5] smart coatings,[6] biomimetic devices,[7] etc. Stimuli-responsive materials rapidly change their thickness, swelling, color, dimension, and/or other physical properties with small changes in the external stimuli such as temperature, pH,[8] light,[9,10] mechanical force,[11] magnetic field,[12] etc. Among those materials, smart thermoresponsive materials have attracted much more attention as they are widely used for various biomedical applications.[13] The most discussed and studied thermoresponsive polymer is poly(*N*-isopropylacrylamide) (PNIPAAm).[14,15] It has a lower critical solution temperature (LCST) of around 32 °C, which is close to body temperature (37 °C), being very useful for biomedical applications.[16] Other example of thermoresponsive polymers are poly(*N*,*N*-diethylacrylamide) (PDEAAm),[17] which has an LCST of 33 °C, and poly(*N*-vinylcaprolactam) (PVCL),[18] which has an LCST of 32 °C, poly[2-(dimethylamino) ethyl methacrylate] (PDMAEMA)[19] with an LCST of around 50 °C and poly(ethylene glycol) (PEG), also known as poly(ethylene oxide) (PEO), whose LCST spans the range from 20 to 90 °C depending on the number of ethylene oxide units

Dr. B. Maiti, A. Abramov, Prof. D. D. Díaz
Institut für Organische Chemie
Universität Regensburg
Universitätsstr. 31, Regensburg 93053, Germany
E-mail: David.Diaz@chemie.uni-regensburg.de
Dr. L. Franco, Prof. J. Puiggalí, Dr. H. Enshaei, Prof. C. Alemán
Departament d'Enginyeria Química
EEBE
Universitat Politècnica de Catalunya
C/Eduard Maristany 10–14, Ed. I2, Barcelona 08019, Spain
The ORCID identification number(s) for the author(s) of this article can be found under https://doi.org/10.1002/adfm.202001683.

DOI: 10.1002/adfm.202001683

Dr. L. Franco, Prof. J. Puiggalí, Prof. C. Alemán
Barcelona Research Center in Multiscale Science and Engineering
Universitat Politècnica de Catalunya
C/Eduard Maristany 10–14, Barcelona 08019, Spain
Prof. J. Puiggalí, Prof. C. Alemán
Institute for Bioengineering of Catalonia (IBEC)
The Barcelona Institute of Science and Technology
Baldiri Reixac 10–12, Barcelona 08028, Spain
Prof. D. D. Díaz
Departamento de Química Orgánica
Universidad de La Laguna
Avda. Astrofísico Francisco Sánchez 3, La Laguna,
Tenerife 38206, Spain
E-mail: ddiazdiaz@ull.edu.es
Prof. D. D. Díaz
Instituto de Bio-Orgánica Antonio González
Universidad de La Laguna
Avda. Astrofísico Francisco Sánchez 2, La Laguna,
Tenerife 38206, Spain

present in the polymer chain.[20] Furthermore, an emerging and important type of thermoresponsive polymers is called shape-memory polymers (SMPs). It is important to mention that shape-memory polymers are also a special class of stimuli-responsive materials, which can spontaneously deform and reform their original shapes upon exposure to temperature as well as to other external stimuli such as pH,[21] light,[22] etc. Shape-memory hydrogels (SMHs) comprise of soft SMP capable of up taking and retaining a large amount of water. In recent years, SMHs have been used in various high-tech applications such as sensors,[23] artificial muscles,[24] actuators,[25] soft robotics,[26] and in vivo treatments.[27] In general, SMHs contain two types of cross-links, one that serves for holding the permanent shape and the other one that is responsible for fixing the temporary shapes, allowing for the recovery of their original shape by formation and breakage of reversible cross-links. In literature, when the shape of the material changes due to a change in temperature, it is called a thermally induced shape-memory effect. The traditional thermoresponsive SMHs usually contain hydrophobic interactions,[28,29] hydrogen bonding, and electrostatic interactions, being the shape-memory effect established on reversible formation and deconstruction of the above mentioned physical interactions upon exposure to heat. Osada and co-workers have synthesized a water swollen shape-memory hydrogel by copolymerizing acrylic acid and *n*-stearyl acrylate (SA), wherein the shape-memory effect was found to be due a reversible order-to-disorder transition of crystalline alkyl groups.[30,31] Gong and co-workers have reported a multistimuli sensitive shape-memory hydrogel consisting of dansyl groups and polyacrylamide, which displayed dual and triple shape-memory properties.[32] The reversible hydrophobic aggregation and disaggregation between dansyl groups in response to the pH or temperature change were found to be responsible for the observed molecular switches. Jiao and co-workers reported a novel SMH made of *N*-vinylpyrrolidone and acryloxy acetophenone (AAP).[33] In this case, reversible formation of π–π interactions among benzene rings in the AAP units were described as responsible for the shape-memory effect. Although there are many studies reported in the literature over the last two decades on thermoresponsive materials and new fabrication techniques, it continues being a great challenge the development of new shape-memory hydrogels, which could meet more complex requirements for different advanced applications.

Herein, we present a new family of thermoresponsive hydrogel membranes by combining a glycerol ethoxylate-based trialkyne and diazide monomers via phototriggered Cu(I)-catalyzed click chemistry. The LCST of the obtained water swollen hydrogel membranes were investigated by differential scanning calorimetry (DSC). As far as we are aware, this is the first time that a glycerol ethoxylate moiety is used to induce a thermoresponsive behavior of polymer membranes depending on the hydrophilic to hydrophobic ratio. In this work, reversible shape-memory effect of the membrane was induced and investigated according to controlled changes in the temperature. Furthermore, swelling and deswelling behaviors of the hydrogel membranes were systematically examined by varying the feed ratio between azide and alkyne monomers. Additionally, thermal properties of the membranes were studied using thermogravimetric analysis (TGA) and DSC. The mechanical properties of the synthesized membranes were studied by UTS measurements. Moreover, the hydrogels showed the ability of absorbing a model dye and releasing it in a controlled manner, which was studied by UV–vis spectroscopy below and above the corresponding LCST value.

2. Results and Discussion

2.1. Synthesis and Characterization of Cross-Linked Membranes

In this study, we employed a photoinitiator, 2,2-dimethoxy-2-phenylacetophenone (DMPA), and a PMDETA copper-chelating click ligand. The photochemical redox reduction of Cu(II) to transiently generated Cu(I) enables the subsequent click reaction.[34] Several cross-linked membranes and polymers P1–P11 were synthesized (**Scheme 1**) by varying both the nature of the azide and alkyne monomers as well as their stoichiometry (**Table 1**).

Figure 1 illustrates the FT-IR spectra of the BA-diazide, trialkyne of glycerol ethoxylate and their corresponding click polymers at different ratio of the components. The transmittance at 2101 cm^{-1} of BA-diazide monomer can be ascribed to the stretching frequency of azide group, whereas the peak at 3245 cm^{-1} and 2114 cm^{-1} corresponds to C—H and —C≡C— bond stretching frequencies of the alkyne groups of the glycerol ethoxylate moiety. In case of P1 and P2 polymers, the alkyne content was significantly high with respect to the equivalent of the azide group in the polymer, resulting in the appearance of a peak at 2114 cm^{-1}. Additionally, for P3 and P4 the azide content was higher with respect to the alkyne content, resulting in the appearance of a peak at 2101 cm^{-1}. Similar characteristic transmittance peaks were found for P5–P8 (Figure S1, Supporting Information). A detailed analysis of the polymer structure was further confirmed by ^{1}H NMR (**Figure 2** and Figure S2, Supporting Information). Figure 2 illustrates the NMR analysis of BA-diazide, trialkyne of glycerol ethoxylate and polymer P2. Successful incorporation of BA-diazide monomer into the copolymers was confirmed from the presence of proton resonances around 6.47, 5.20 ppm, corresponding to the aromatic proton along with the additional triazole signal at 7.8 ppm in the ^{1}H NMR spectra of the polymer. To establish the versatility of the membrane preparation method, we also synthesized some other polymers comprising different types of azide and alkynes (Scheme 1).

2.2. Thermoresponsive Behavior of Membranes

Since PEG-based polymers exhibit thermoresponsive behaviors, we also expected to observe a similar response in our resulting cross-linked membrane.[35,36] The LCSTs of the cross-linked membranes were measured by DSC and the results are summarized in **Figure 3**. Exothermic peaks in the thermograms represent the LCST where heat is required to break the intermolecular hydrogen bonds between water molecules and polymer chains. Figure 3 indicates that the LCST of P1 is higher compared to P3. Similar results were also obtained for P9 and P11. It is expected that the incorporation of more hydrophobic comonomers or cross-linker will decrease the

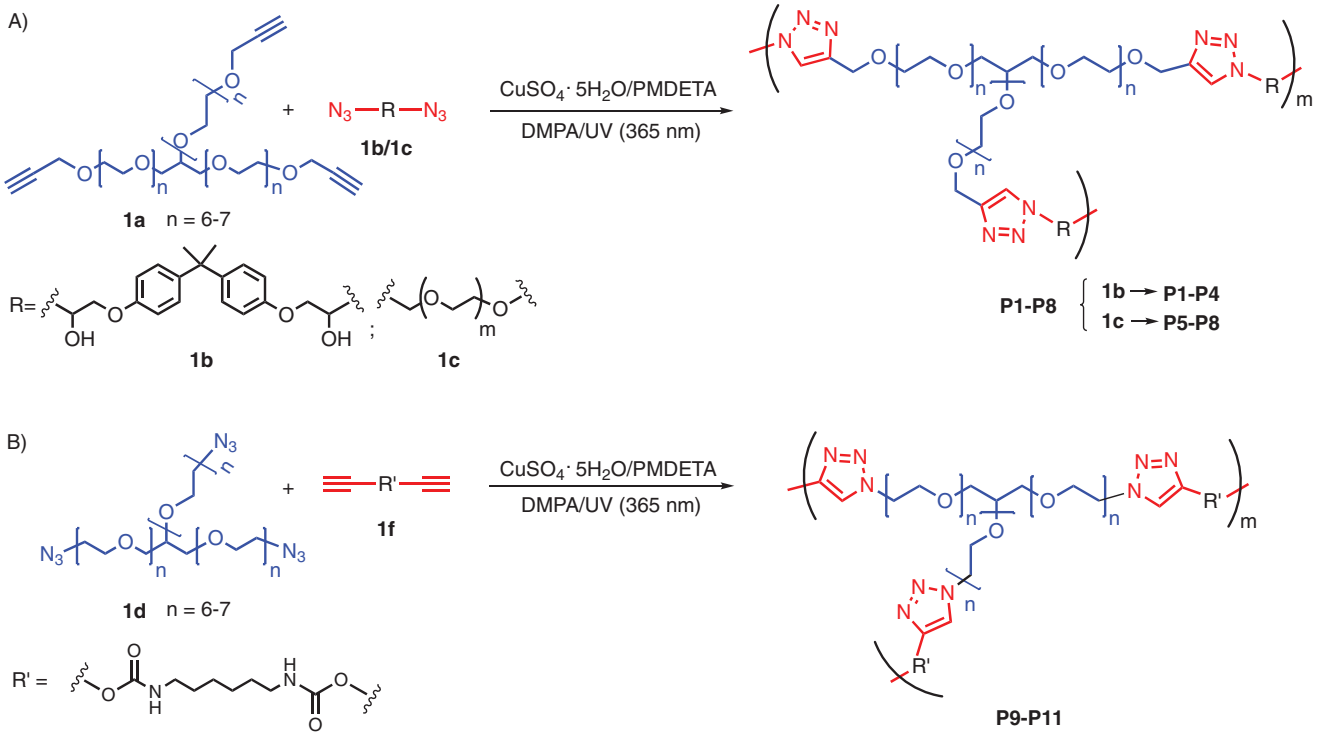

Scheme 1. Synthesis of glycerol ethoxylate-based cross-linked polymers P1–P11 via Cu(I)-assisted azide-alkyne photoclick reaction.

amount of intermolecular hydrogen bonding, resulting in less heat being required for breaking the hydrogen bonds, resulting in a decrease of the LCST. However, in our case the cross-linking density was found to influence the LCST of the synthesized hydrogels. In case of P1 and P9 cross-linking density is more than P3 and P11 as more amount of cross-linker (**1a**) was used for P1 and P9. The distance between interacting segments of polymer chains decreased with increasing the cross-link density of the membrane, which enhances the repulsive hydration forces resulting in decrease of the LCST.[37,38]

In contrast, in the case of polymers P5–P8, we observed no phase transition below 80 °C as both the azide (PEG_{600}) and trialkyne (**1a**) were hydrophilic and we could not go beyond this temperature due to the slow evaporation of water. Additionally, polymers such as P2 and P10 were water soluble and LCST was determined by UV–vis spectroscopy (Figure S3, Supporting Information). We observed that the solution was slowly

Table 1. Summary of different click reactions carried out in this work.

Polymer[a)]	Alkyne: azide ratio	Nature of the polymer	LCST [°C]	T_g	SR_e [%]
P1	1:1	Cross-linked membrane	41[b)]	–27.9	99
P2	1:0.5	HB polymer	39.2[c)]	–41.7	–
P3	0.5:1	Cross-linked membrane	44.6[b)]	–7.2	45
P4	0.2:1	HB polymer	–	–4.3	–
P5	1:1	Cross-linked membrane	ND[b)]	–47.5	1035
P6	1:0.5	HB polymer	ND[c)]	–41.9	–
P7	0.5:1	Cross-linked membrane	ND[b)]	–48.3	375
P8	0.2:1	HB polymer	ND[c)]	–52.9	–
P9	1:1	Cross-linked membrane	30.6[a)]	–38	140
P10	0.5:1	HB polymer	41[b)]	–54	–
P11	1:0.5	Cross-linked membrane	53.7[a)]	–22	71

[a)]Different polymers made by click reaction. Abbreviations: HB, hyperbranched polymer; ND, not determined; [b)]LCST determined from DSC; [c)]LCST determined from and UV–vis.

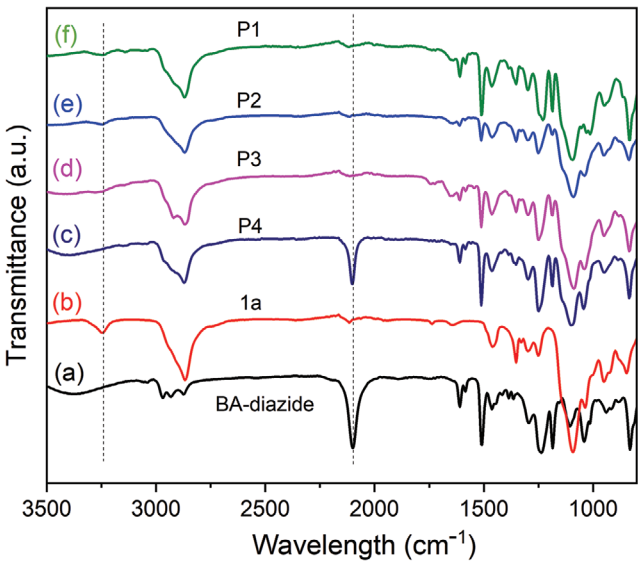

Figure 1. FT-IR spectra of a) BA-diazide, b) **1a**, c) P4, d) P3, e) P2, and f) P1.

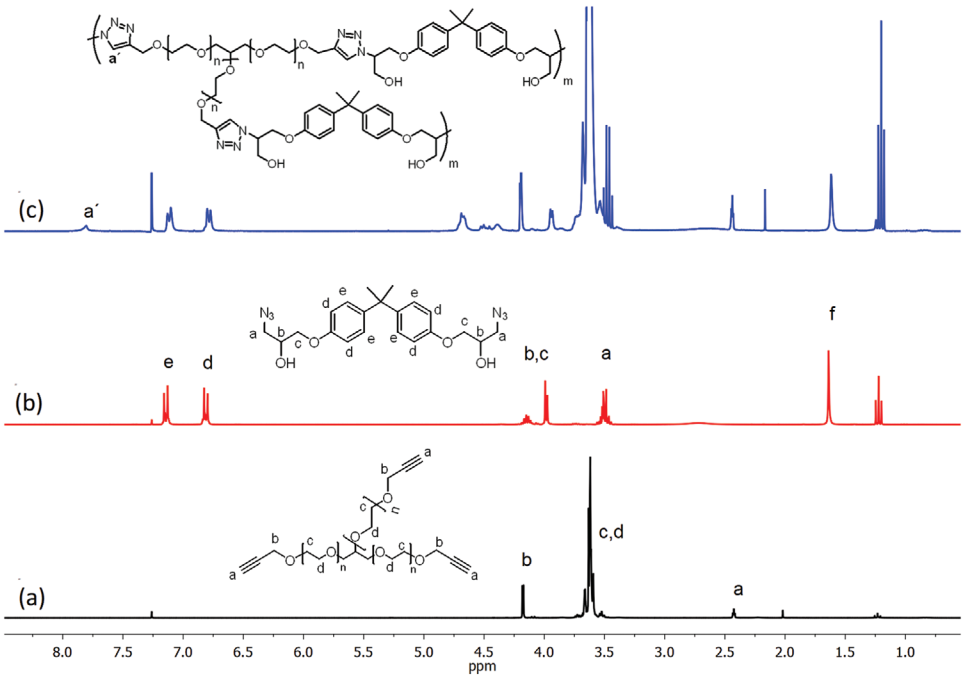

Figure 2. ^{1}H NMR spectra of a) trialkyne, b) BA-diazide, and c) HB polymer (P2) in $CDCl_3$.

transformed from transparent to opaque by increasing the temperature, according to a thermoresponsive response of the polymers due to the glycerol ethoxylate moiety. In case of polymer P6, no LCST was observed due to the presence of glycerol ethoxylate as well as PEG (600 g mol^{-1}) moieties, which increases the overall hydrophilicity of the polymer.

2.3. Swelling Kinetics

The swelling ratios (SR_e) of different sets of cross-linked membranes were investigated in deionized (DI) water at 22 °C. SR_e were calculated using Equation (1) at room temperature by placing a weighed amount of the hydrogel in water for 24 h to reach the equilibrium swelling. Then, the swelled gel was taken out from the water, wiped with moist tissue paper and weighed (**Figure 4**). The SR_e values of all the hydrogels are represented in Table 1. As shown in Figure 4a, the P1 gel showed higher SR_e compare to P2 membrane due to the presence of higher content of hydrophilic glycerol ethoxylate moiety. A similar trend was also found for P8 and P10 gel where P8 gel showed higher SR_e compared to P10 membrane (Table 1 and Figure S4, Supporting Information). It is also important to mention that in case of P5, where both the azide and alkyne were hydrophilic, the gel showed ten times more SR_e than P1 and P9 having the same azide and alkyne ratio. **Figure 5** shows how the size of the membrane increased after swelling.

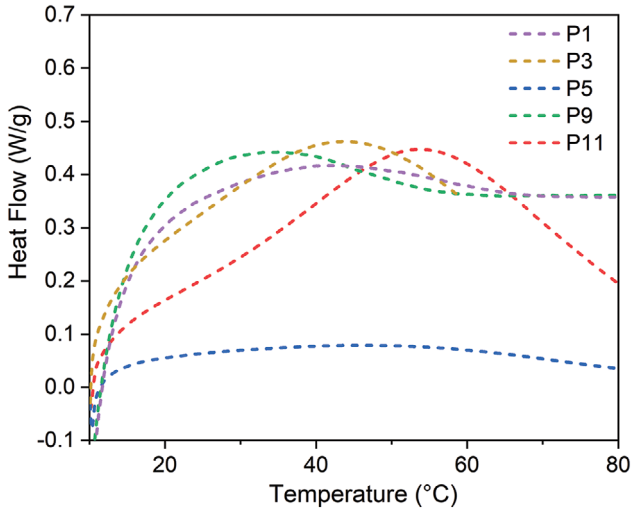

Figure 3. DSC curves of different hydrogel membranes.

2.4. Deswelling Kinetics

The deswelling of hydrogel membranes are shown in **Figure 6**. The deswelling kinetics of previously swollen hydrogel samples were studied by examining the % of water retention as a function of the water absorption time in hot water (50 °C). The plots indicate that the deswelling rate of the hydrogel samples obviously depends on the feed ratio of the two different monomers. For all the membranes, the water retention dropped quickly in the early stage of heating and then decreased slowly since the driving force for deswelling was gradually reduced upon the dehydration of the gels and reached its maximum. It is worth noting that membranes having higher amount of glycerol ethoxylate moiety had a stronger affinity for water molecules, while also acting as a water-releasing channel when dehydration happened, thereby helping the network to shrinkage more sufficiently. For example, after 60 min, the water retention of

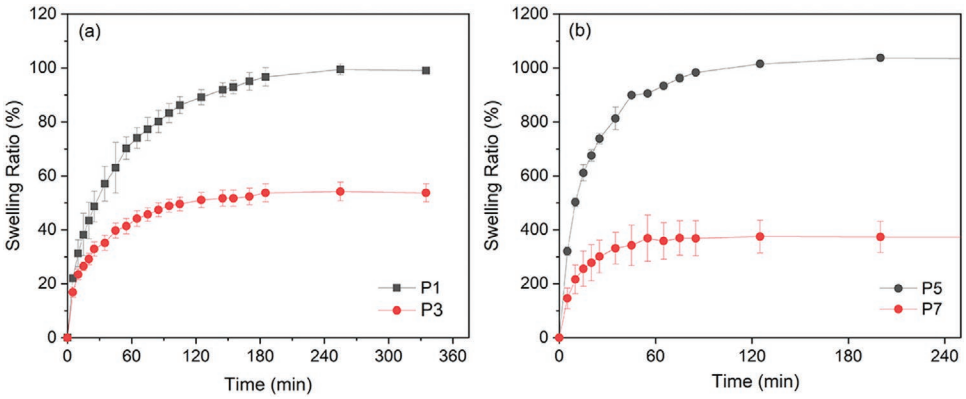

Figure 4. Comparison of equilibrium swelling ratios for a) P1 and P3, and b) P5 and P7 at 22 °C as a function of time.

the P3 hydrogel was reduced to about 50%, whereas that of P1 hydrogel reached a steady-state value of 30% (Figure 6). Similarly, P9 hydrogel was reduced to about 50%, whereas that of P11 hydrogel reached a steady-state value of 30%. Additionally, the thermosensitive deswelling behavior of the membranes is also due to the alternation in hydrophilicity to hydrophobicity of the polymer network. On immersion of P1/P3 hydrogel into hot water at 50 °C, the outside region of the membrane would be affected first and the hydrophobic interactions among the hydrophobic groups in the outmost region become stronger, resulting in a rapid shrinkage of the outmost surface and a formation of a dense skin layer. Once this skin layer is formed, the free water molecules in the membrane are prevented from diffusing out, which results in the slow response rate.[39,40] However, the incorporation of the hydrophilic chains, glycerol ethoxylate moiety, could inhibit the formation of the dense skin layer, and the hydrophilic chains act as releasing channels for water molecules when the collapse occurs.[41] The more glycerol ethoxylate moiety is introduced into the hydrogel network, the more water releasing channels would be formed. Therefore, the deswelling rate increases with the increase of the glycerol ethoxylate moiety content from P3 to P1.

2.5. Thermal Properties

The TGA and derivative thermogravimetric curves (DTGs) were used to determine the thermal behavior such as weight loss, residual char level, etc., at a certain temperature. The degradation behavior of cross-linked membranes was investigated by TGA analysis (**Figure 7**) and summarized in Table S1 (Supporting Information). As shown in Figure 7, for P6 and P8, the initial weight loss step seen below 200 °C is mostly due to the loss of other solvent or water absorbed by the hygroscopic membrane. The major weight loss took place in between 300 and 400 °C, may be due to the degradation of the 1,2,3-triazole moiety and polymer backbone.[42] However, in case of P4 and P8 polymers, we observed a degradation peak at 252 °C (Figure 7b) maybe due to the presence of small residues of unreacted excess of BA-diazide.

The influence of different stoichiometry of azide and alkyne during polymerization on the glass transition temperature of the dried membrane was determined by differential scanning calorimetry and the results are summarized in **Figure 8**. For instance, the T_g of P1, P2, P3, and P4 are –27.9, –41.7, –7.2, and –4.3 °C, respectively. The value of glass transition temperature (T_g) of the polymer is summarized in Table 1 and it depends on the mobility/flexibility of the polymer chain, i.e., the higher the flexibility, the lower the T_g is. In our materials, the mobility of the polymer chain depends on the amount of glycerol ethoxylate moiety present in the membrane. In the case of P1 and P2 the amount of glycerol ethoxylate moiety is higher compared to P3 and P4, and the amount of glycerol ethoxylate chain is present in the following order P2 > P1 > P3 > P4 (Table 1). However, for P5 to P8 polymers, we used both glycerol ethoxylate (1000 g mol^{-1}) and divalent PEG (600) as trialkyne and diazide components, respectively. Herein, divalent PEG (600) is more flexible than glycerol ethoxylate. In case of polymers P5 to P8, divalent PEG (600) is in the driver seat to control the mobility of the polymer chain. The amount of divalent PEG (600) chain is present in the following order P8 > P7 > P5 > P6, while T_g values follow an inversed order (–52.9 °C < –48.3 °C < –47.5 °C < –41.9 °C) (Table 1).

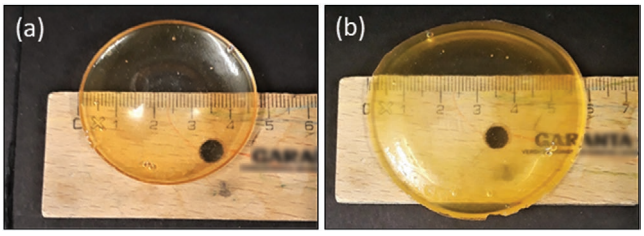

Figure 5. a) P1 membrane before and b) after swelling in water after 24 h.

2.6. XRD Analysis of the Membranes

Furthermore, the amorphous structure of the membranes was confirmed by wide-angle X-ray scattering (WAXS; Figure S5, Supporting Information), which showed diffraction peaks at $2\theta = 20.14$ for P3, 20.9 for P2, P5, and P11, respectively.

2.7. Tensile Testing of the Membranes

Tensile testing was performed in order to investigate the mechanical properties of the synthesized membranes

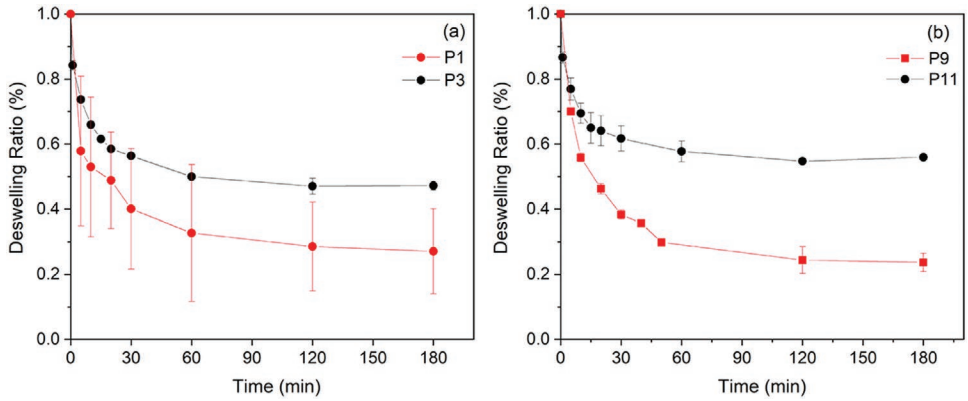

Figure 6. Comparison of water retention upon deswelling of different membranes: a) P3 and P1, b) P11 and P9.

(**Figure 9**). To measure the tensile properties of the cross-linked membrane, with varying % glycerolethoxylate moiety, the membranes were subjected to axial loading at a constant crosshead speed (5 mm min^{-1}) until failure. From an average of five replicas with independent specimens for each membrane, the Young's modulus (E), elongation at break (ε_{break}), and ultimate tensile strength (UTS) of the materials were determined and summarized in **Table 2**.

In general, the mechanical strength of P3 was found to be much better than that of P1 and P7 (Figure 9), exhibiting higher tensile strength and young modulus. This can be attributed to the percentage of hard segment, which was higher for P3 than for P1, or to the rigidity of such segment when percentages are identical, which is higher for P3 than for P7. As expected, the rigidity and percentage of the hard segment affects the elongation capacity, which was lower for P3 than for P1 and P7. Despite these observations, the strain capacity of P3 was higher than 80%, evidencing that the elasticity is significant. Differences between P9 and P11 were ascribed to the cross-linking degree. Thus, the strength of these membranes increases with the cross-linking degree, while the elongation capacity decreases. As expected, the mechanical properties of P9 and P11 were comparable to those of P7 and P3, respectively. It should be noted that all these systems are formed from flexible azide monomers and, therefore, their mechanical performance is predominantly influenced by the cross-linking degree. The

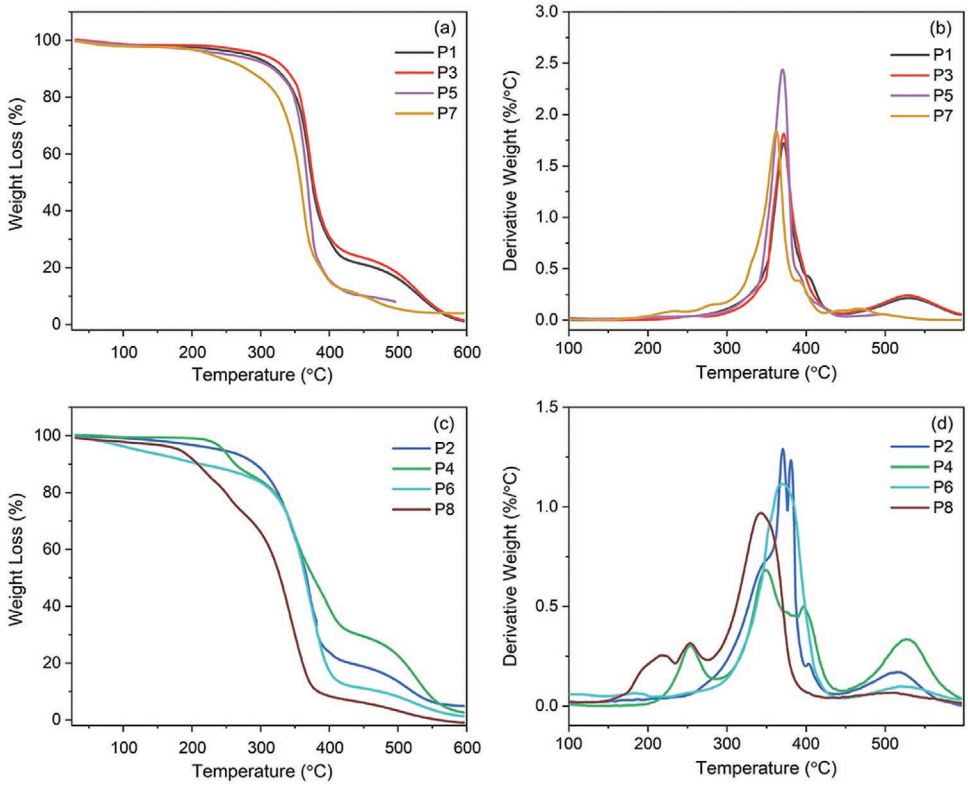

Figure 7. a) TGA and b) DTG thermograms of different polymers.

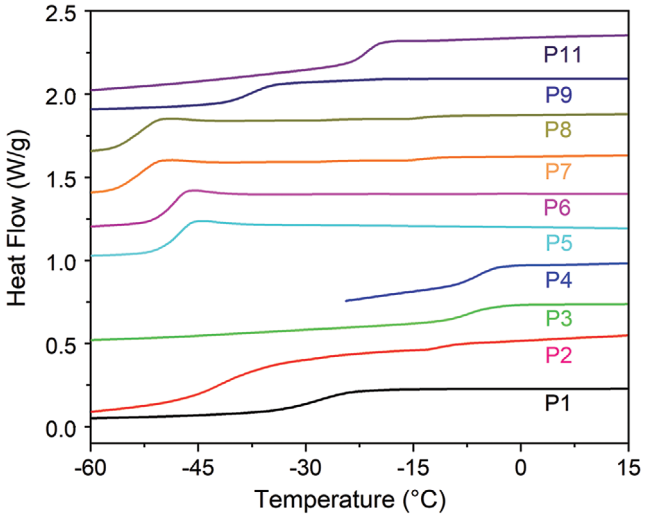

Figure 8. DSC plots of dry cross-linked membranes and polymers.

elongation at break (Figure 9b) and, especially, the Young modulus (Figure 9c) were higher than those typically observed for lyophilized hydrogel membranes.

2.8. Thermoresponsive Shape-Memory Properties

In general, shape-memory hydrogel membranes can display two different types of cross-links. One constitutes a covalent network, which is responsible to maintain their permanent shape. The other type is a physical reversible network, which is able to fix their temporary shape. In this investigation we have applied phototriggered Cu(I)-catalyzed click chemistry to fix the original shape and weaker the hydrogen bonds between polymer chains and water molecules, as well as hydrophobic-hydrophobic interactions between the polymer chains act as reversible interactions to provide shape-memory and shape recovery properties. To study the thermoresponsiveness of our system, the membrane was immersed into DI water for 24 h. Then, the swollen membrane was placed in hot water (50 °C) resulting in a bending actuation (**Figure 10** and movie in the Supporting Information). When we placed the membrane once again in cold water (22 °C), the membrane returned to its original state within 45 s. At a temperature below the transition temperature, hydrogen bonding interactions between the polymer chain and water molecules serve to lock a permanent shape of the swollen membrane, whereas above the critical temperature, hydrogen bonds were weakened and the hydrophobic-hydrophobic attractions predominated, resulting in a collapse and aggregation of macromolecular chains. Herein, we were able to control and repeat the shape-memory for at least 5 cycles. As shown in Figure 9 and in the video (Supporting Information), the shape recovery took place very quick with a recovery time below 50 s, achieving completely reproducible shape-memory effects.

2.9. Dye Absorption and Dye Release Study

It is well known that stimuli-responsive polymeric materials can be used for the controlled release of encapsulated molecules. This prompted us to test our thermoresponsive hydrogel membranes as temperature-controlled delivery systems using rhodamine B (RB) as a model dye. To load RB inside the hydrogel membranes, a small piece of the desired dried hydrogel film was placed inside a 2 mL (1×10^{-5} M) solution of RB, and the absorbance was recorded at different time intervals. **Figure 11**a shows that the dye absorption capacity increased with increasing time, reaching the equilibrium after 24 h. Specifically, the dye absorption efficiency of P1 was 86% after 24 h. Additionally, in vitro release of absorbed RB in PBS (pH 7.4) solution was evaluated over time at two different temperatures, below (37 °C) and above LCST (50 °C). The results showed a slightly higher % release for P1-based membrane at 50 °C compared to that obtained at 37 °C (Figure 11b).[43,44]

3. Conclusions

In this study, we have successfully synthesized a series of thermoresponsive, rigid and strong SMHs containing a trialkyne derivative of glycerol ethoxylate via Cu(I)-catalyzed photoclick reaction. To the best of our knowledge, this is the first report describing the use of glycerol ethoxylate moiety to induce a controlled thermoresponsive behavior depending on the feed ratio of other hydrophobic comonomers (azides) during the click photopolymerization. The gel with the highest content of hydrophilic glycerol ethoxylate moiety showed the highest SR_e. We proposed that the observed shape-memory effect is due to

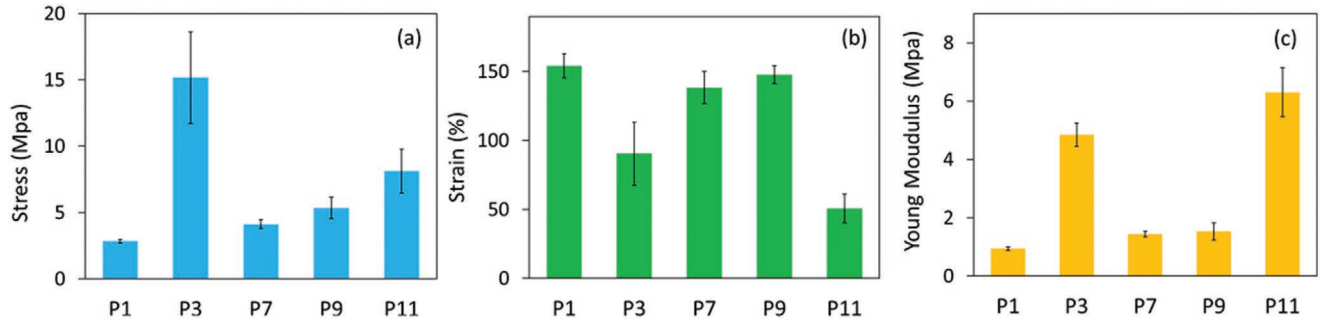

Figure 9. Variation of the a) stress at break, b) elongation at break, and c) Young's modulus with different membranes.

Table 2. Comparison of tensile properties of different membranes.

Membrane	E [MPa]	ε break [%]	σ [MPa]
P1	0.9 ± 0.1	154 ± 9	2.8 ± 0.1
P3	4.8 ± 0.4	91 ± 23	15.2 ± 3.4
P7	1.4± 0.1	138 ± 12	4.1 ± 0.3
P9	1.5 ± 0.3	148 ± 6	5.3 ± 0.8
P11	6.3 ± 0.8	51 ± 10	8.1 ± 1.6

the reversible formation and breakage of the hydrogen bonds between water molecules and polymer chains, as well as the hydrophobic interactions between polymer chains, in response to the temperature. We also investigated the release of an encapsulated model dye below and above the LCST, being the percentage of released dye much faster above the LCST compared to that obtained below LCST. We believe that this strategy will help to increase the list of tunable shape-memory hydrogels and promote the design of novel shape-memory systems for different biomedical applications.

4. Experimental Section

Materials: All reagents and solvents were purchased from commercial suppliers and used as received: Glycerol ethoxylate (average $M_n = 1000$ g mol^{-1}), polyethylene glycol ($M_n = 600$ g mol^{-1}), sodium azide (≥ 99.5%), sodium hydride (60% dispersed in mineral oil), propargyl bromide (80%), hexamethylene diisocyante (≥ 99%), and $CuSO_4{\cdot}5H_2O$ (98%) were purchased from Sigma-Aldrich. Bisphenol A diglycidylether (BPA, 98%), 2,2-dimethoxy-2-phenylacetophenone (DMPA, > 98%) and *N*,*N*′,*N*″,*N*‴-pentamethyldiethylenetriamine (PMDETA, > 98%) were purchased from TCI Europe. Methanesulfonoyl chloride (98%) was purchased from Alfa Aesar. Triethyl amine (Et_3N, ≥ 99%) and ammonium chloride (NH_4Cl, ≥ 99.5%) were purchased from Merck.

Instrumentation: Blak-Ray B100 UV lamp was used to perform the photoclick reactions. ^{1}H NMR spectra were acquired in a Bruker 300 spectrometer operating at 300 MHz at 25 °C. FT-IR (Cary 630) spectroscopy was carried out on a spectrometer, equipped with a Diamond Single Reflection ATR-System. DSC studies were performed on TA Instruments Q100 series (TA instruments, New Castle, DE, USA) with Tzero technology equipped with a refrigerated cooling system (RCS, TA instruments, New Castle, DE, USA). Calibration of the DSC was performed with indium and sapphire disks. Runs were conducted at 10 °C min^{-1} from room temperature to 150 °C, under a flow of dry nitrogen using a sample weight of ≈5 mg. Mettler Toledo DSC1 STARe at 10 °C min^{-1} from room temperature to 150 °C. Thermogravimetric (TGA) and differential thermogravimetric (DTGA) data were acquired with a Q50 thermogravimetric analyzer of TA Instruments (New Casttle, DE, USA) under air atmosphere at a heating rate of 10 °C min^{-1}. Rigaku Smart Lab powder diffractometer having Cu Kα = 1.54059 Å radiation was used for recording X-ray diffraction (XRD) spectra. The UV–vis spectroscopic study was carried out using a Perkin-Elmer Lambda 35 UV–vis spectrophotometer.

Synthesis of Cross-Linked Membranes: In a typical example, compound **1a** (0.28 mmol, 0.30 g), compound **1b** (0.28 mmol, 0.122 g), $CuSO_4{\cdot}5H_2O$ (2 mol% of **1a**) PMDETA (2 mol% of **1a**), and DMPA (4 mol% of **1a**) were dissolved in MeOH (1.5 mL). Subsequently, the maximum amount of methanol was removed under vacuum and the sample was irradiated with UV light (365 nm) for 10 min followed by annealing at 100 °C for 3 h. Then, the obtained hydrogel was washed by using 0.02 M ethylenediaminetetraacetic acid (EDTA) disodium salt solution overnight to remove the Cu salt (note: EDTA disodium salt solution was replaced by fresh solution three to four times during this period until

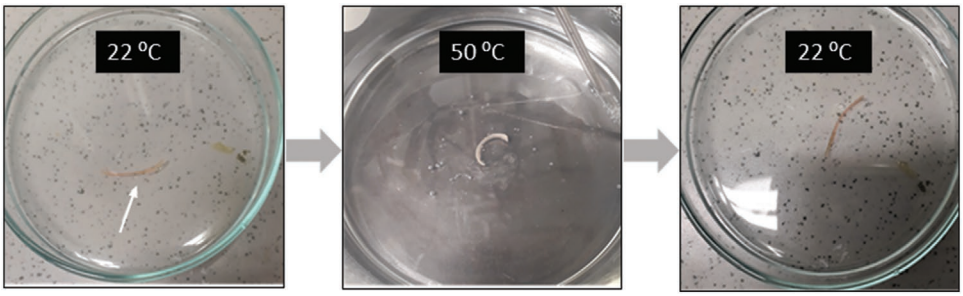

Figure 10. Photographs that represent the macroscopic temperature induced shape-memory behavior of P1 membrane.

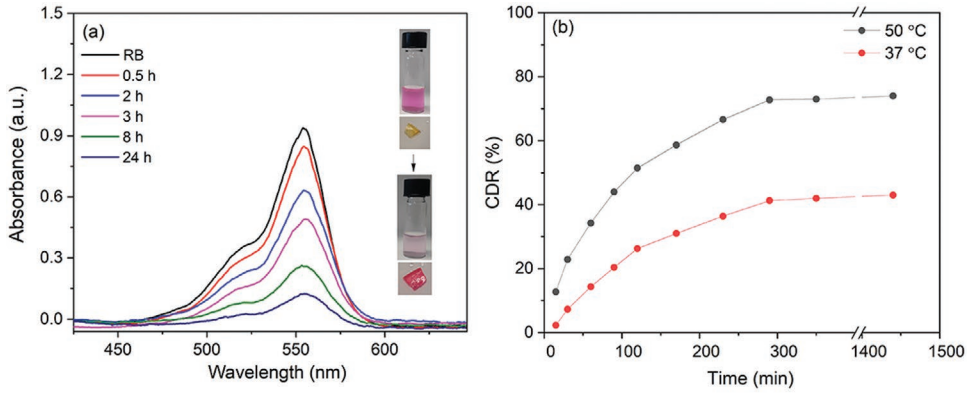

Figure 11. a) UV–vis dye absorption spectra at different times. b) Drug release at different temperatures (37 and 50 °C) in PBS buffer (pH 7.4).

no more blue color due to the extraction of metal ions was observed). Subsequently, the membrane was repeatedly washed with DI water and dried in a vacuum oven at 90 °C for 2 d.

Determination of LCST: The LCSTs of the hydrogel membranes were measured using DSC. Membranes were allowed to swell completely for at least 24 h in DI water. The membrane surface was gently wiped with wet tissue paper to remove the extra water. The sample was sealed in the T-zero pan and the mass was noted and carefully placed along with a reference pan on the heater. Samples were then heated from room temperature to 70 °C at a rate of 2 °C min^{-1} under a dry nitrogen atmosphere. For water soluble polymers, 2 mg mL^{-1} polymer solution was prepared and transferred to a UV cuvette. Then, the turbidity of the solution was measured using a UV–vis spectrophotometer by monitoring the % transmittance (%T) changes at λ = 500 nm. The temperature was slowly increased from 25 to 70 °C and equilibrated the sample for 5 min at the measurement temperature and the %T value at 500 nm was recorded. The LCST was identified where a reduction of 50%T of the polymer solution was noticed.

Measurement of Swelling Kinetics: The equilibrium SR_e is defined as the ability to absorb water by the gel matrix with respect to its dry weight until a constant value is reached. The swelling behavior of the hydrogel membranes was studied by gravimetric analysis at room temperature (22 °C). A small piece of the corresponding hydrogel membrane was placed in a 20 mL vial and immersed in DI water. Then, the swollen hydrogel membrane was carefully taken out from the vial, wiped with wet tissue paper to remove the excess surface water and weighed on a dry glass Petri dish at different time intervals. The SR_e was calculated using Equation (1)

$$\text{Swelling ratio}\,(SR_e\%) = \frac{W_t - W_d}{W_d} \times 100 \quad (1)$$

where W_t corresponds to the weight of the swollen hydrogel at time t and W_d is the weight of the dry hydrogel.

Measurement of Deswelling Kinetics: The deswelling study was carried out gravimetrically above the LCST of the hydrogel membranes. Typically, a small piece of the hydrogel was first immersed in water at 22 °C until the equilibrium swelling was reached. The equilibrated hydrogels were immediately transferred to a hot water bath at 50 °C. Then, the hydrogels were taken out from the hot water at different time intervals and weighed after wiping off the excess surface water by moist tissue paper. The deswelling study of each sample was carried out at least two times and the values were averaged. A small piece of swollen hydrogel, after reaching the equilibrium swelling at 22 °C, was transferred to beakers containing hot water at 50 °C. At different time intervals, the weight of the hydrogel was determined after wiping off the excess surface water by moist tissue paper. Water retention was calculated by using Equation (2)

$$\text{Water retention} = \frac{W_t - W_d}{W_0 - W_d} \quad (2)$$

where W_t is the weight of the hydrogel at time t and W_0 is the weight of the swollen hydrogel below the LCST at equilibrium.

Tensile Testing: Mechanical properties were evaluated with a Zwick Z2.5/TN1S testing machine with integrated testing software (testXpert, Zwick). The deformation rate for stress-strain assays was 5 mm min^{-1}. Dog bone shaped tensile specimens were prepared for measurements according to the following dimensions: overall length, 30 mm; gage length, 10 mm; width, 1 mm. Measurements were done at least five times for each sample, results being averaged and the corresponding standard deviations considered. An important factor in mechanical tests is good sample grip, which is particularly difficult when the specimens are formed by sticky and soft hydrogel membranes. The strategy used to overcome this challenge includes the utilization of elastic materials to help grip the samples (i.e., to reduce the pressure of grip).

Dye Absorption and Dye Release Study: A known amount of the hydrogel membrane was placed into a 20 mL vial containing 2 mL of RB aqueous solution (1×10^{-5} M). The concentration of RB in the solution was recorded at constant intervals of time using a UV–vis spectrophotometer at a wavelength of 560 nm. The final concentration of the dye in the solution was calculated according to the Beer-Lambert law ($A = \varepsilon \cdot c \cdot l$, where A is the absorbance of the dye at a certain absorption wavelength in solution, ε is the molar extinction coefficient, and l is the path length of the incident light). The final concentration of the dye in the solution was obtained by the Beer–Lambert equation, which ultimately determined the color removal efficiency (RE) of the dye via Equation (3)

$$\%CRE = \frac{C_i - C_f}{C_i} \times 100 \quad (3)$$

where C_i represents the initial concentration of the dye in the solution and C_f corresponds to the final concentration of the dye in the presence of the adsorbing gel.

For drug release study, a known amount a preswollen dye-absorbed hydrogels was first rinsed with PBs buffer (1 mL) and placed into a vial containing fresh PBS buffer (2 mL). The vials containing the hydrogels were transferred to a 50 °C or 37 °C water bath and the absorbance of the solution was determined at different time intervals.

Supporting Information

Supporting Information is available from the Wiley Online Library or from the author.

Acknowledgements

The authors acknowledge Universität Regensburg, MINECO/FEDER (RTI2018-098951-B-I00 and RTI2018-101827-B-I00), the Agència de Gestió d'Ajuts Universitaris i de Recerca (2017SGR359 and 2017SGR373), and B. Braun Surgical, S.A. for financial support. C.A. is grateful for the support in research to ICREA Academia program for excellence in research. D.D.D. thanks the DFG for the Heisenberg Professorship Award and the Spanish Ministry of Science, Innovation and Universities for the Senior Beatriz Galindo Award (Distinguished Researcher; BEAGAL18/00166).

Conflict of Interest

The authors declare no conflict of interest.

Keywords

hydrogels, membranes, photoclick, polymers, shape-memory, thermoresponsive

Received: February 22, 2020
Revised: March 26, 2020
Published online: April 24, 2020

[1] Q. Zhang, N. R. Ko, J. K. Oh, *Chem. Commun.* **2012**, *48*, 7542.
[2] A. P. Blum, J. K. Kammeyer, A. M. Rush, C. E. Callmann, M. E. Hahn, N. C. Gianneschi, *J. Am. Chem. Soc.* **2015**, *137*, 2140.
[3] X. Hu, Y. Zhang, Z. Xie, X. Jing, A. Bellotti, Z. Gu, *Biomacromolecules* **2017**, *18*, 649.
[4] R. Ravichandran, S. Sundarrajan, J. R. Venugopal, S. Mukherjee, S. Ramakrishna, *Macromol. Biosci.* **2012**, *12*, 286.
[5] M. R. Islam, Y. Gao, X. Li, M. J. Serpe, *J. Mater. Chem. B* **2014**, *2*, 2444.
[6] J. E. Stumpel, D. J. Broer, A. P. Schenning, *Chem. Commun.* **2014**, *50*, 15839.

[7] H. Yang, W. R. Leow, T. Wang, J. Wang, J. Yu, K. He, D. Qi, C. Wan, X. Chen, *Adv. Mater.* **2017**, *29*, 1701627.
[8] S. Dai, P. Ravi, K. C. Tam, *Soft Matter* **2008**, *4*, 435.
[9] Y. Zhao, *Macromolecules* **2012**, *45*, 3647.
[10] J. F. Gohy, Y. Zhao, *Chem. Soc. Rev.* **2013**, *42*, 7117.
[11] D. A. Davis, A. Hamilton, J. Yang, L. D. Cremar, D. Van Gough, S. L. Potisek, M. T. Ong, P. V. Braun, T. J. Martínez, S. R. White, J. S. Moore, *Nature* **2009**, *459*, 68.
[12] J. Thévenot, H. Oliveira, O. Sandre, S. Lecommandoux, *Chem. Soc. Rev.* **2013**, *42*, 7099.
[13] M. A. Ward, T. K. Georgiou, *Polymers* **2011**, *3*, 1215.
[14] M. Heskins, J. E. Guillet, *J. Macromol. Sci., Part A: Chem.* **1968**, *2*, 1441.
[15] K. Jain, R. Vedarajan, M. Watanabe, M. Ishikiriyama, N. Matsumi, *Polym. Chem.* **2015**, *6*, 6819.
[16] Y. Guan, Y. Zhang, *Soft Matter* **2011**, *7*, 6375.
[17] Z. Song, K. Wang, C. Gao, S. Wang, W. Zhang, *Macromolecules* **2016**, *49*, 162.
[18] M. N. Mohammed, K. B. Yusoh, J. H. B. H. Shariffuddin, *Mater. Express* **2018**, *8*, 21.
[19] E. Karjalainen, V. Aseyev, *Macromolecules* **2014**, *47*, 2103.
[20] J. F. Lutz, *J. Polym. Sci., Part A: Polym. Chem.* **2008**, *46*, 3459.
[21] X. J. Han, Z. Q. Dong, M. M. Fan, Y. Liu, J. H. Li, Y. F. Wang, Q. J. Yuan, B. J. Li, S. Zhang, *Macromol. Rapid Commun.* **2012**, *33*, 1055.
[22] D. Iqbal, M. Samiullah, *Materials* **2013**, *6*, 116.
[23] X. Li, M. J. Serpe, *Adv. Funct. Mater.* **2016**, *26*, 3282.
[24] S. M. Mirvakili, I. W. Hunter, *Adv. Mater.* **2018**, *30*, 1704407.
[25] L. Viry, C. Mercader, P. Miaudet, C. Zakri, A. Derre, A. Kuhn, M. Maugey, P. Poulin, *J. Mater. Chem.* **2010**, *20*, 3487.
[26] L. Hines, K. Petersen, G. Z. Lum, M. Sitti, *Adv. Mater.* **2017**, *29*, 1603483.
[27] C. Wang, H. Yue, Q. Feng, B. Xu, L. Bian, P. Shi, *ACS Appl. Mater. Interfaces* **2018**, *10*, 29299.
[28] J. Hao, R. Weiss, *ACS Macro Lett.* **2013**, *2*, 86.
[29] Y. Wang, K. A. Burke, *Soft Matter* **2018**, *14*, 9885.
[30] Y. Osada, A. Matsuda, *Nature* **1995**, *376*, 219.
[31] A. Matsuda, J. Sato, H. Yasunaga, Y. Osada, *Macromolecules* **1994**, *27*, 7695.
[32] X. L. Gong, Y. Y. Xiao, M. Pan, Y. Kang, B. J. Li, S. Zhang, *ACS Appl. Mater. Interfaces* **2016**, *8*, 27432.
[33] C. Jiao, Y. Chen, T. Liu, X. Peng, Y. Zhao, J. Zhang, Y. Wu, H. Wang, *ACS Appl. Mater. Interfaces* **2018**, *10*, 32707.
[34] B. J. Adzima, Y. Tao, C. J. Kloxin, C. A. DeForest, K. S. Anseth, C. N. Bowman, *Nat. Chem.* **2011**, *3*, 256.
[35] D. Roy, W. L. Brooks, B. S. Sumerlin, *Chem. Soc. Rev.* **2013**, *42*, 7214.
[36] B. Maiti, S. Maiti, P. De, *RSC Adv.* **2016**, *6*, 19322.
[37] M. Milichovsky, *J. Biomater. Nanobiotechnol.* **2010**, *1*, 17.
[38] T. Ikeda-Fukazawa, N. Ikeda, M. Tabata, M. Hattori, M. Aizawa, S. Yunoki, Y. Sekine, *J. Polym. Sci., Part B: Polym. Phys.* **2013**, *51*, 1017.
[39] J. Chen, M. Liu, S. Chen, *Mater. Chem. Phys.* **2009**, *115*, 339.
[40] U. Haldar, M. Nandi, B. Maiti, P. De, *Polym. Chem.* **2015**, *6*, 5077.
[41] Y. Kaneko, R. Yoshida, K. Sakai, Y. Sakurai, T. Okano, *J. Membr. Sci.* **1995**, *101*, 13.
[42] A. Movahedi, K. Moth-Poulsen, J. Eklöf, M. Nydén, N. Kann, *React. Funct. Polym.* **2014**, *82*, 1.
[43] O. Werzer, S. Tumphart, R. Keimel, P. Christian, A. M. Coclite, *Soft Matter* **2019**, *15*, 1853.
[44] Y. Tian, Y. Liu, B. Ju, X. Ren, M. Dai, *RSC Adv.* **2019**, *9*, 2268.